Article

System Identification of Mosques Resting on Soft Soil. The Case of the Suleiman Mosque in the Medieval City of Rhodes, Greece

Anna Karatzetzou *, Dimitris Pitilakis ^{ID} **and Stella Karafagka** ^{ID}

Civil Engineer Department, Aristotle University of Thessaloniki, 54124 Thessaloniki, Greece; dpitilak@civil.auth.gr (D.P.); stellak@civil.auth.gr (S.K.)
* Correspondence: akaratze@civil.auth.gr

Abstract: The present study focuses on the dynamic system identification of the Suleiman Mosque minaret in the medieval city of Rhodes, Greece. Suleiman Mosque was built in 1522 at the site of the destroyed Christian Church of the Apostles. First, we performed sets of ambient vibration measurements at the minaret of the monument. Based on these data, we calculated the eigenproperties of the minaret. Next, we modeled the monument in three dimensions, using the finite element method. Six numerical models were considered. Model I is the simplest one (isolated, fixed base minaret). Model VI is the most complicated one (simulation of the whole mosque also considering soil–structure interaction and foundation flexibility). The calculated predominant periods and mode shapes of Models I–VI are validated against the microtremor field measurements, recorded on the minaret's two floors and ground level. We elaborate on the reliability of finite element models for earthquake response evaluation, considering soil–structure interaction and foundation flexibility on the mode shape eigenfrequencies. Additionally, we discuss the seismic response of the minaret compared to the whole monument. We observed no significant difference in the first two modes of response, implying that the minaret's dynamic behavior is slightly affected by the entire mosque's presence.

Keywords: microtremors; field measurements; monuments; ambient vibration measurements; modal analysis; time history analysis

1. Introduction

Currently, there is an urgent need to promote efficient, safe, and cost-effective strategies for the risk assessment and mitigation of historical masonry monuments [1]. Preservation of cultural heritage assets must guarantee their capacity to last over time against decay, natural hazards, and extreme events without losing their authenticity and usability. The assessment of historical buildings' structural health through non-destructive techniques, which allow for taking measurements with no damage to the building and without interfering with its regular use, is fundamental to preserving their cultural integrity. For this purpose, structural health monitoring (SHM) plays a crucial role in providing information on structures' dynamic properties and accurately evaluating monuments' seismic response.

In the last decade, the number of SHM systems designed and implemented on historic structures increased considerably [2–4]. Ambient noise measurement is one of the most widespread methodologies for identifying structures' dynamic properties [5–8]. Among the numerous recent publications on microtremor measurements, we mention the following: (a) System identification techniques using ambient noise measurements to estimate natural structural frequencies, vibration modes, mode shapes, and damping [9–11]. (b) Frequency domain techniques also using ambient noise measurements in historical masonry structures to estimate the actual structural pathology of different structural components [12,13] and the natural frequencies of the monument [5–7,14,15]. (c) Array measurement of microtremors has been widely used to estimate the elastic dynamic soil properties in terms of shear-wave velocity, using various techniques [16–19]. During ambient vibration

testing, the structure is triggered by loads such as the wind or human activity. Thus, the structure behaves in the elastic range. Comparing the field measurements with the results of numerical analyses such as modal analysis is a way to upgrade the simulation of a structure and consider the effects of the soil properties in its dynamic response. Thus, the data obtained from microtremor measurements can be used to estimate the monument's fundamental dynamic properties, namely the frequencies, the modes of vibration, and the modal damping ratios. This information helps to develop reliable numerical models and supports the effective planning and prioritization of strengthening interventions to monumental structures. Furthermore, the ambient noise's broad frequency content, without an artificial excitation, is crucial for recognizing the main modal frequencies in a single step. In general, operational modal analysis (OMA) is more often applied than forced vibration measurements because the same modal parameters can be obtained from vibration data in operational rather than laboratory conditions [20]. Several studies have been conducted using ambient vibration testing for the identification of the dynamic behavior [21–23] and vulnerability assessment [24,25] of buildings.

In this study, we investigate the Suleiman Mosque situated in the medieval city of Rhodes, in Greece. Particular emphasis is given to the seismic response of the minaret of the Suleiman Mosque. We performed sets of ambient vibration measurements. Minarets are slender structures and generally built near mosques using different structural materials such as brick, stone, concrete, timber, and steel. They can be classified depending on the slenderness ratio [26]. Masonry minarets are most vulnerable to earthquakes due to their slender geometry [27–29]. The seismic behavior of minarets depends on soil type, boundary conditions, geometrical characteristics, mechanical properties of units, and wind and earthquake loads. Due to the large number of collapses occurring due to earthquake effects, minarets' seismic performances have been widely investigated in the literature. Experimental and numerical behaviors of masonry and reinforced concrete minarets or towers with and without restoration were investigated by Şahin et al. [30], Osmancikli et al. [31], Bayraktar et al. [32], Bernardeschi et al. [33], Bayraktar et al. [34], and Forcellini et al. [35]. Although there are several studies on the SSI effect on buildings, the studies taking into account the SSI effect on minarets or towers are very limited. To this end, we study the effect of soil–structure interaction and foundation flexibility on the dynamic characteristics of minarets.

Dynamic soil–structure interaction (SSI) effects are usually neglected in most studies. However, SSIs may have a substantial impact on the seismic response of structures, modifying their dynamic characteristics and seismic performance at the foundation level [36–39]. The seismic vulnerability of slender minarets and towers may be heavily influenced by the interaction with the foundation soil subjected to strong ground motions. Casolo et al. [28] conducted comparative seismic vulnerability analysis on ten masonry towers to identify the factors that play a crucial role in their seismic vulnerability, while Hökelekli and Al-Helwani [40] investigated the effects of SSIs with infinite elements on the seismic damage behavior of stone masonry minarets with different soil types, considering the linear behavior of the soil domain. Several other studies also deal with the influence of soil–structure interactions on the fragility of buildings either on shallow or deep foundations [41–44].

The main objectives of the present paper are (i) to discuss the reliability of finite element models (compared with the experimental data) to evaluate the actual mode shapes and eigenfrequencies of the minarets and thus to evaluate the response of the minarets to potential ground motions in future earthquakes, (ii) to discuss the effect of soil–structure interactions and foundation flexibility on the dynamic characteristics of minarets, (iii) to discuss the response of the minaret compared to the whole monument and highlight the finding that the minaret responds independently from the rest of the structure. The present paper provides solid evidence of the unique dynamic response of soil–mosque–minaret systems, using both numerical and experimental data, highlighting the effect of the soil on the dynamic response.

Initially, we describe the historical data of Suleiman Mosque, its geometrical and mechanical properties, as well as the soil properties of the area where the monument is located. Subsequently, we present the field microtremor surveys performed, as well as the system identification and OMA we conducted. Six numerical models are presented and separately studied. In general, it is seen that due to the symmetry of the minaret, the first and second frequency values are almost the same for all the examined numerical models. This also implies that the seismic behavior of the minaret dominates the whole mosque's seismic response.

2. The Suleiman Mosque in the Medieval City of Rhodes

2.1. Historical Data

Suleiman Mosque, located in the medieval city of Rhodes (Figure 1), was built in the 16th century by Sultan Suleiman the Magnificent, just after the conquest of Rhodes in 1522 (Figure 2a). It is said that the sultan built the monument in 1522 to celebrate the victory of the Turkish over the Knights. The present study's subject is mainly the minaret of the Suleiman Mosque and not the whole structure. The 26 m tall minaret with its two balconies stands at the northwest side of the monument's central hall. Many natural disasters, the most important of which are earthquakes and an explosion underneath the bell tower of a nearby church, damaged the monument. In the early 1980s, the minaret started declining. For this reason, rebuilding of the minaret was unavoidable (Figure 2b) due to the advanced decay of its sandstone blocks. In 1988, the minaret was dismantled and then rebuilt in 2005. The masonry of the new structure was built from fine quality local limestone (more robust than the former masonry stone blocks) and lime mortar with 10% concrete content, reproducing the original sculptured moldings and reinforced with horizontal metal hoops, vertical titanium pins, and lead poured between each course of the masonry [45].

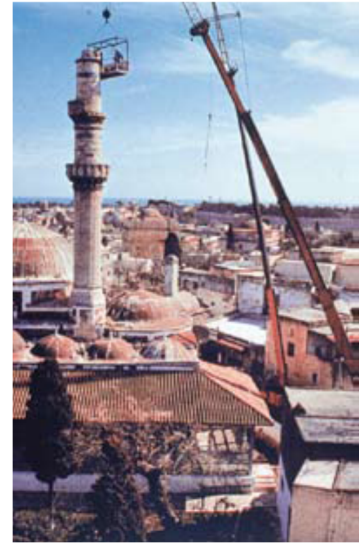**Figure 1.** The medieval city of Rhodes (Google maps).

2.2. Geometrical Properties

The mosque is made of load-bearing masonry. The mosque's plan view is symmetrical in the NW–SE axis and includes three square spaces in a row. The central space, 8.00×8.00 m, is the largest one, while the other two have a plan view of approximately 5.00×5.00 m. The three spaces are lined so that the northwest side, which is also the façade, is about 22.00 m. The masonry, internal and external, is about 1.00 m thick. All three areas are vaulted. The central space has a total height of approximately 15.00 m, while the other two spaces have a height of about 10.00 m. The information regarding the structural geometry of the mosque was provided by Dellas et al. [46]. The typical external configuration of a minaret in height includes the following parts (Figure 3):

i. the square part of the base of the minaret (kaide);
ii. the transitional part of the conversion of the square cross-section into a cylinder cross-section (küp);
iii. the cylindrical section up to the first balcony, which continues higher if there are more balconies;
iv. the balconies (şerefe);
v. the cylindrical or polygonal section above the last balcony (petek);
vi. the conical part (külah); and
vii. the decorative ending part (alem).

(**a**)   (**b**)

Figure 2. (**a**) Suleiman Mosque of the medieval city of Rhodes, (**b**) rebuilding of the minaret due to the advanced decay of its sandstone blocks [46].
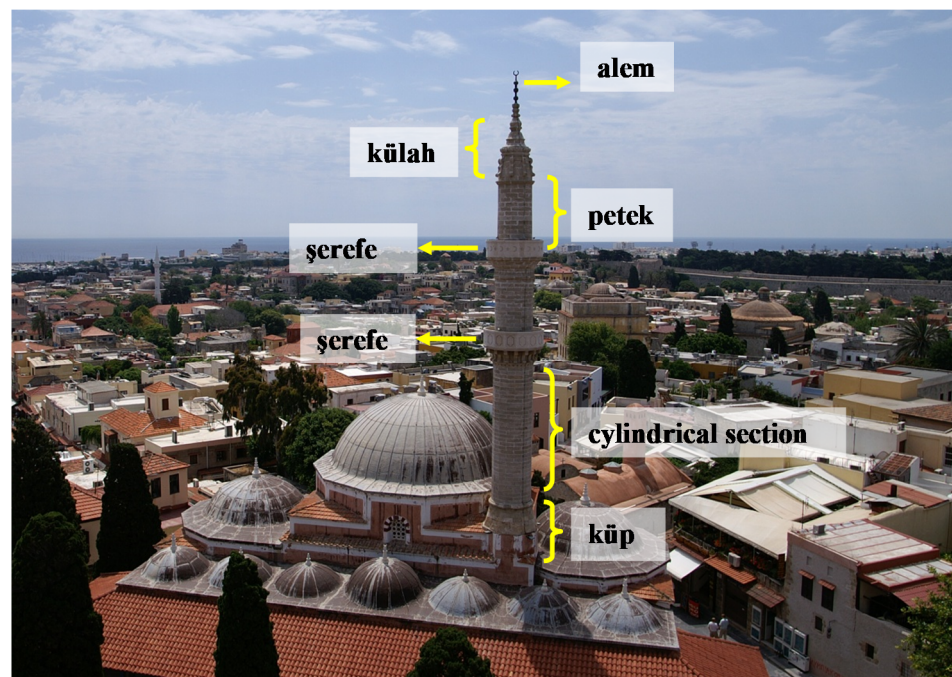

Figure 3. Description of the external typical parts of a minaret in height (modified after [46]).

The minaret base stands at +8.55 m from the ground surface (+0.00), while the top of the minaret at +34.50 m. The section at the bottom (+8.55) of the minaret up to +11.60 m is octagonal (section A-A). The external radius is equal to 2.80m at the base and 2.20 m at +11.60 m. The internal radius is equal to 1.40 m. At the first balcony (+19.83 m) level, the section is cyclic with an external radius equal to 2.20 m and a width of masonry equal to 0.30 m. The cross-section remains cyclic from the first balcony up to the top of the structure (+29.00 m). The external radius is reduced up to 1.80 m. Figure 4 shows the architectonic façade of the minaret and its cross-sections.
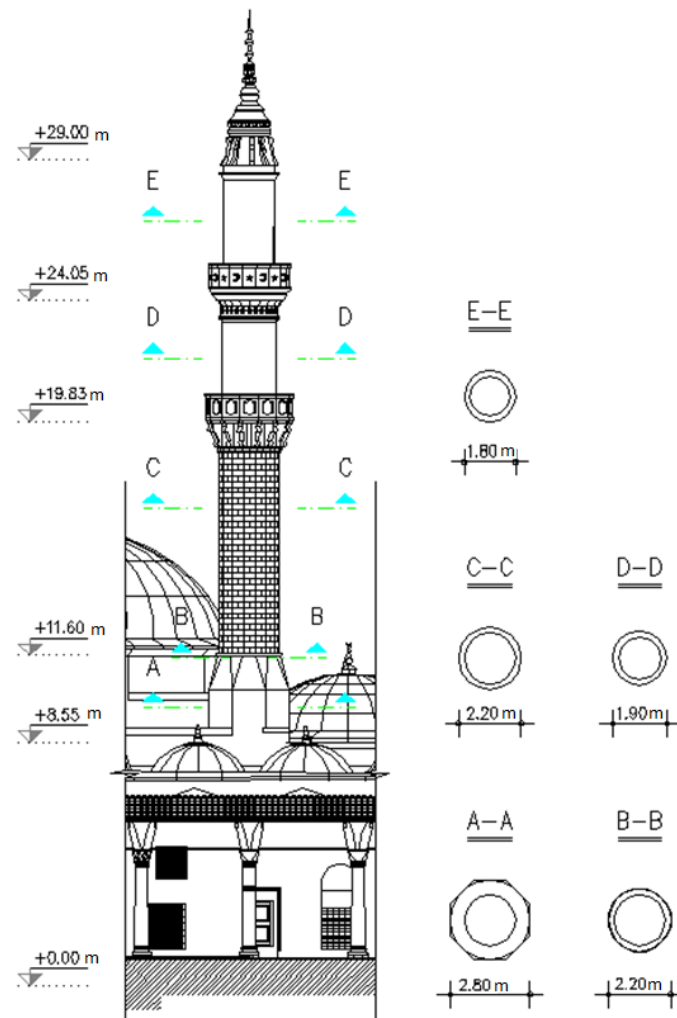

Figure 4. Architectonic façade and cross-sections.

2.3. Masonry Properties

The mosque and the minaret are constructed with ashlar masonry of limestones. Table 1 shows the material properties of the mosque and the minaret. The minaret and the mosque density are 22 kN/m^3 and 20 kN/m^3, respectively. Simultaneously, the modulus of elasticity is equal to 6 GPa for the minaret and 3 GPa for the mosque. Finally, the compression strength of the minaret is equal to 11.5 MPa and the compression strength of the mosque is equal to 2.5 MPa. This significant difference between the compression strengths of the limestone of the mosque (2.5 MPa) and the minaret (11.5 MPa) can be attributed to the fact that the herein selected properties of the minaret concern the new construction, which was built in 2005 (see Section 2.1). The assumed material properties stem from laboratory studies conducted in [47] and utilized in the numerical analyses performed during the restoration of the minaret [45]. It is noted that, according to the EC8 provisions, in the numerical analyses, the masonry elastic modulus should be reduced

by 50% (cracked condition, stage II). However, as proposed by Chatzidakis [45], for the numerical configurations, we utilize here the initial material properties, as they stem from laboratory tests.

Table 1. Material properties of the mosque and the minaret.

	Minaret	Mosque
material	limestone	limestone
γ (kN/m^3)	22	20
Ewc (GPa)	6	3
fwc (MPa)	11.5	2.5

2.4. Soil Properties

The geotechnical information from past geotechnical studies and surveys in the medieval city of Rhodes consists of 17 sampling boreholes. According to [48], the city is divided into four geotechnical zones. The characteristics of each zone are summarized in Figure 5. The geotechnical map of Rhodes (Figure 5), was also validated in 2011 through a comprehensive campaign of field microtremor surveys, which were performed in the medieval city of Rhodes [49]. It is obvious that the geotechnical information, in terms of shear-wave velocity, contributes only to the description of the surface soil materials, since it is limited to the upper 40.0 m, but for the needs of the present study this is sufficient, as we simulate the soil using appropriate static, linear elastic springs and thus the only parameter we need for the soil is the shear-wave velocity V_s for the first 30 m of the soil profile and Poisson's ratio ν. To this end, for the Suleiman Mosque, which is located in Zone II according to Figure 5 or in soil class C according to the EC8 soil characterization scheme [50], the $V_{s,30}$ was assumed equal to 270 m/s (the average value for soil class C) and Poisson's ratio ν was assumed equal to 0.33.
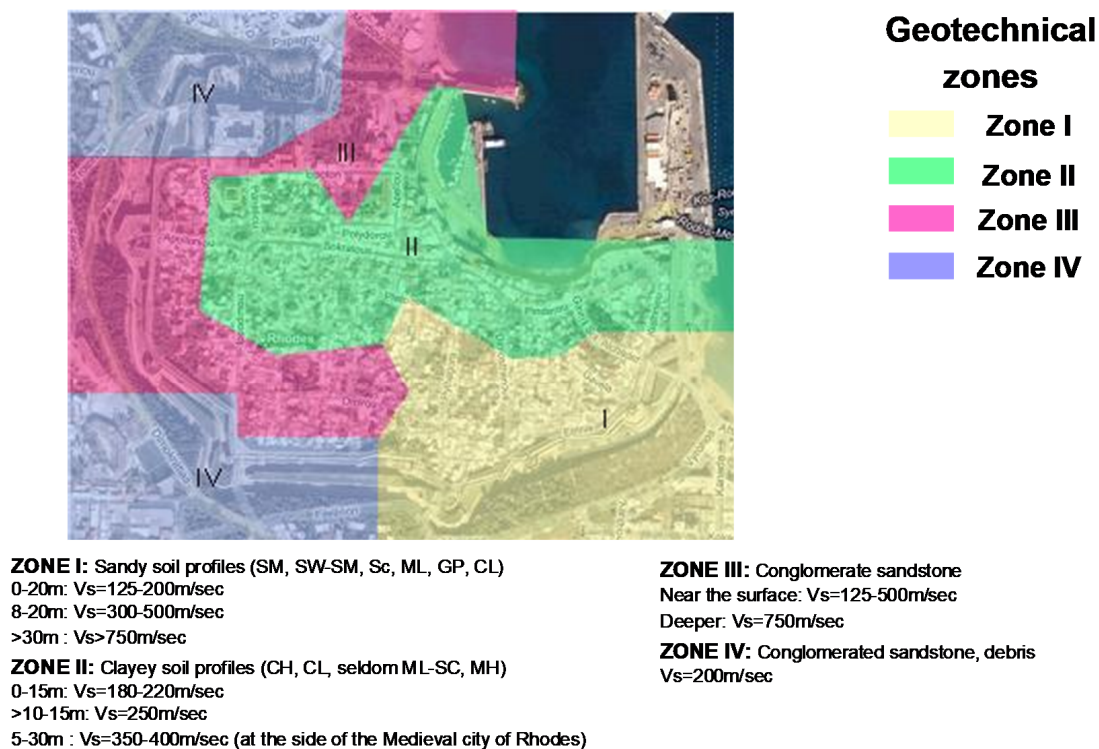

Geotechnical zones

Zone I
Zone II
Zone III
Zone IV

ZONE I: Sandy soil profiles (SM, SW-SM, Sc, ML, GP, CL)
0–20m: Vs=125-200m/sec
8–20m: Vs=300-500m/sec
>30m : Vs>750m/sec

ZONE II: Clayey soil profiles (CH, CL, seldom ML-SC, MH)
0–15m: Vs=180-220m/sec
>10-15m: Vs=250m/sec
5–30m : Vs=350-400m/sec (at the side of the Medieval city of Rhodes)

ZONE III: Conglomerate sandstone
Near the surface: Vs=125-500m/sec
Deeper: Vs=750m/sec

ZONE IV: Conglomerated sandstone, debris
Vs=200m/sec

Figure 5. Geotechnical map of Rhodes [48].

3. System Identification and Operational Modal Analysis

To evaluate the structure's response, the so-called modal model is required, which expresses the structure's dynamic behavior. System identification builds a modal model of a physical system based on experimental data [51]. By knowing the observed system response (output data) to an excitation source (input data), a parametric modal model can be obtained, defined by a set of modal parameters (eigenfrequencies/eigenperiods, mode shapes, damping ratios). Ambient vibration measurements are usually used to perform OMA and identify the structure's modal parameters. Different stochastic identification techniques extract a structural system's modal parameters, namely the parametric and non-parametric methods. In parametric methods, the dynamic characteristics are extracted based on a parametric model updated to fit the recorded data. In contrast, in non-parametric ones, the modal parameters are estimated directly by post-processing the measured data. We used the short-term ambient noise measurements to derive the experimental modal model of the Suleiman Mosque minaret, located in the medieval city of Rhodes, Greece, and identify its modal properties based on OMA. We used the modal identification results to determine the optimal analytical model, which presents peculiarities, as it is a high-rise structure made of load-bearing masonry.

3.1. Mictrotremor Measurements

In the framework of the PERPETUATE project [52], we performed a comprehensive campaign of field microtremor surveys in the medieval city of Rhodes. Concerning the minaret of Suleiman Mosque, we conducted single station HVSR ambient noise measurements [53]. The temporary experiment's scope was to define the site characteristics (fundamental frequency and amplification of resonance) of the main geological/geotechnical formations of the area and the dynamic characterization of the minaret in terms of eigenfrequencies and mode shapes. The ambient noise was recorded for 15 and 20 min using a one broadband triaxial Guralp seismometer CMG-40T connected to a Reftek recording system (DAS-130) and a GPS unit. The noise data were analyzed using Nakamura's technique. Noise windows of 200 to 400 s in duration were selected, avoiding obvious parasites (spikes) from external noises (cars, machines, pedestrians). These windows were divided into smaller windows of 20 to 40 s in duration with 50% overlapping between the adjacent windows. Each window (total number 19 to 39) was 10% cosine tapered, and Fourier transformed, and its amplitude spectrum smoothed using a Hanning function. The transfer function of each window was calculated, as well as its average. The coordinates of their first maximum peak correspond to the dominant frequency and amplification of each investigated site. Even though the HVSR ratio's amplitude does not give the real amplification potential of a future strong seismic excitation due to different reasons [54], its estimated values may be used in a qualitative way to characterize the relative differences in amplification between investigated sites.

On the contrary, there is no doubt about the accuracy of the measured resonant frequency. Moreover, the amplification factor may validate the resonant frequency's reliability. The greater the amplification, the more accurate the resonant frequency is. Resonant frequencies with measured amplification factors greater than 3.0 are generally considered accurate.

We placed the instruments on the first and second floor of the minaret, and on the ground soil, just outside the mosque (Figure 6). The average HVSR was estimated to be around 3.0–4.0. A second peak appeared on HVSR ratios from 1.34–1.47 Hz with amplitude lower and/or equal to 3.0. On the minaret's first floor, the frequency was calculated between 0.39 and 0.41Hz with an amplification greater than 9.0. A second peak appeared with amplitude between 10 and 20 at 1.6 Hz. On the second floor, the measured frequency was 1.63 Hz, while the amplification factor was between 40 and 100 in both horizontal components (Figure 7).

Figure 6. The instruments were placed on the ground soil and on the two balconies of the minaret [52].
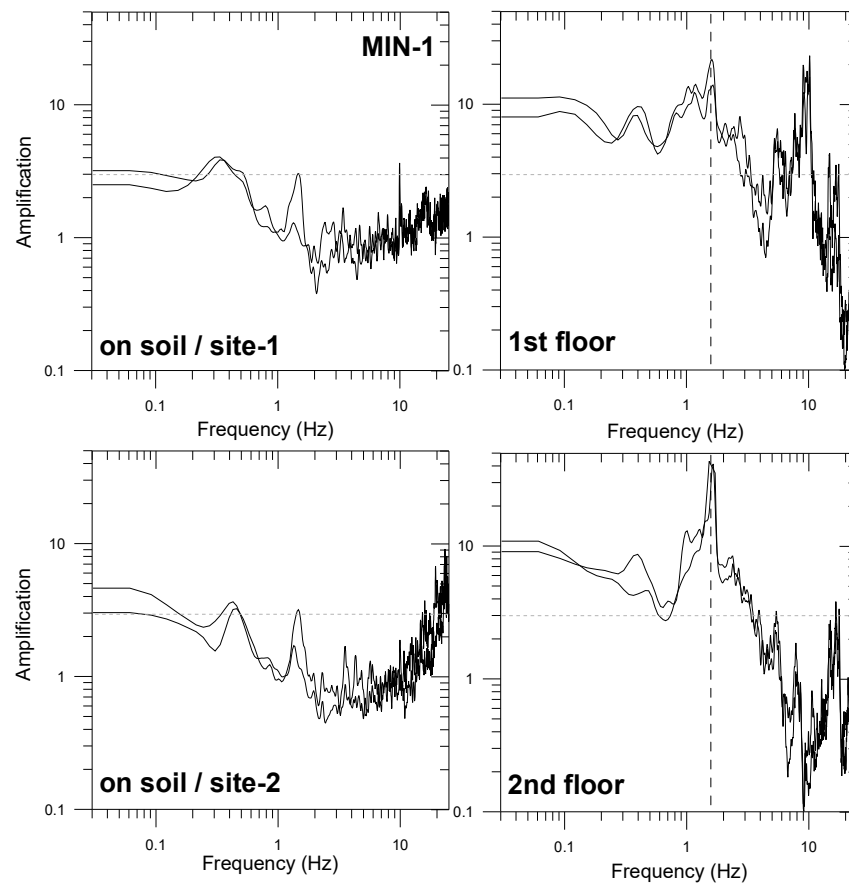

Figure 7. Average HVSR ratios at Suleiman Mosque on the soil and the two floors of the minaret [52].

3.2. Operational Modal Analysis Using Ambient Noise Measurements

Field monitoring data can be used to represent the actual state of a structure better, reducing uncertainties associated with its modeling properties, including non-physical parameters, such as aging effects and structure maintenance. The use of building monitoring

data constitutes an essential tool for the identification of the actual structure properties based on system identification and OMA [20].

We assessed the minaret's dynamic characteristics using single station HVSR measurements. We employed i) parametric stochastic subspace identification (SSI) [55], ii) the non-parametric peak picking (PP) identification technique [56], and iii) the frequency domain decomposition (FDD) [57] methods to perform OMA and extract the natural frequencies/periods and the mode shapes of the structural system, using MACEC 3.3 software [58]. We used both the horizontal (longitudinal and transverse) and the ambient noise's vertical components.

In the parametric methods, modal identification is conducted by applying the reference-based covariance-driven SSI method. The latter involves selecting a mathematical space state model where the parameters are adjusted to fit the measured data. This model calibration aims to minimize the deviation between the predicted and measured system response. A common approach in the modal analysis is to over-specify the model order. The system's physical modes are separated from the noise modes. This separation is performed manually in a stabilization diagram. The selection of the model order for constructing the stabilization diagrams for the SSI method depends on the number of modes of interest and the number of sensors. Herein, we selected a model order range from 2 to 60 in steps of two. The goal was to use this diagram to detect the columns of stable modes that satisfy the defined stabilization criteria and continuously select a representative mode from each column.

In the non-parametric methods, system identification is based on estimating the positive power spectral density (PSD+) matrix at discrete frequency lines. For the PSD+ calculation of the measured outputs collected from all channels, we applied the correlogram method. In the PP method, the average normalized PSD (ANPSD) is calculated. The well-separated modes are estimated by picking the peaks in the ANPSD. In the FDD method, which is considered an improved version of the PP method, the singular values are obtained from the PSD matrix decomposition. The modal parameters are computed by picking the peaks of the first singular value.

The results of the parametric and non-parametric analyses for the minaret are presented in Figure 8. Table 2 also summarizes the modal identification results in terms of eigenfrequencies for the minaret computed with the three system identification methods for two time windows. Comparing the results between the three techniques (SSI, PP, and FDD), we observe that the estimated frequency values for the three well-separated modes are very close to each other (practically the same for the first three modes) for the three identification methods applied. The damping values extracted using the SSI technique and presented in Table 2 appear consistent with the level of vibration for the first and second modes. On the contrary, high damping estimates are obtained for the third mode, namely 1.79% and 3.11%. This indicates that the higher modes' estimates may have been affected by biases. They do not reflect the ranges under operational conditions generally reported in seismic design and engineering manuals [59,60].

Table 2. Modal identification results for the minaret estimated using parametric SSI and non-parametric PP and FDD identification techniques.

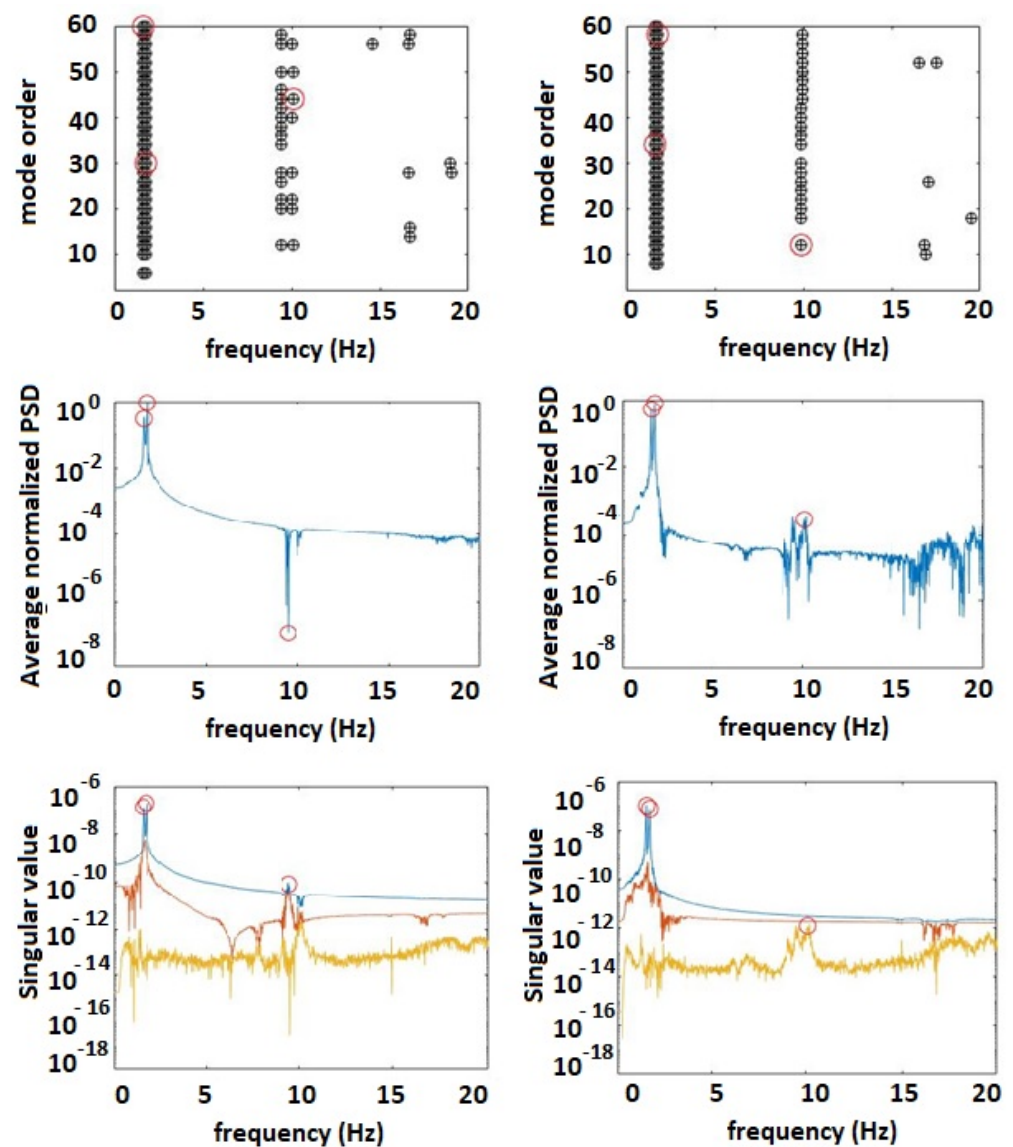| Time Window	Mode	SSI		PP	FDD
		f (Hz)	Damping (%)	f (Hz)	f (Hz)
1	1	1.63	0.57	1.62	1.63
	2	1.80	0.51	1.80	1.80
	3	10.09	1.79	9.48	9.46
2	1	1.65	0.63	1.65	1.65
	2	1.82	0.56	1.82	1.82
	3	9.88	3.11	10.09	10.09

Figure 8. Identification results through OMA for the minaret based on the SSI (**top**), PP (**middle**), and FDD (**bottom**) methods.

4. Results and Discussion

4.1. Numerical Investigation

Parametric modal analyses were performed in SAP2000 software [61] using the finite element method (FEM). The numerical models were composed of elastic beam column elements and shell elements (Figure 9). SAP2000 software allows the use of surface finite elements (shell elements), quadrilateral or triangular, with four and three nodes, respectively, which are considered suitable for the simulation of buildings of load-bearing masonry. For all examined numerical models (Models I-IV), which will be described in the following section, the only load is the weight of construction (static permanent load). We evaluated the first twelve eigenmodes. For the modal analyses, the mass was calculated from the self-mass of the elements.

To simulate the minaret, two different numerical models were constructed using finite elements. The first model (Figure 9a) is a fixed base cantilever column with distributed mass. The structure, in this case, is fixed at the level of +8.55 m, and the base of the minaret is not modeled. The cantilever column, which is 21.25 m in height (we modeled up to the level of 29.80 m, Figure 4), is modeled with 18 beam elements. The second model

(Figure 9b) simulates the whole mosque. The structure is modeled from the level of 0.00 m up to 21.25 m (Figure 4).
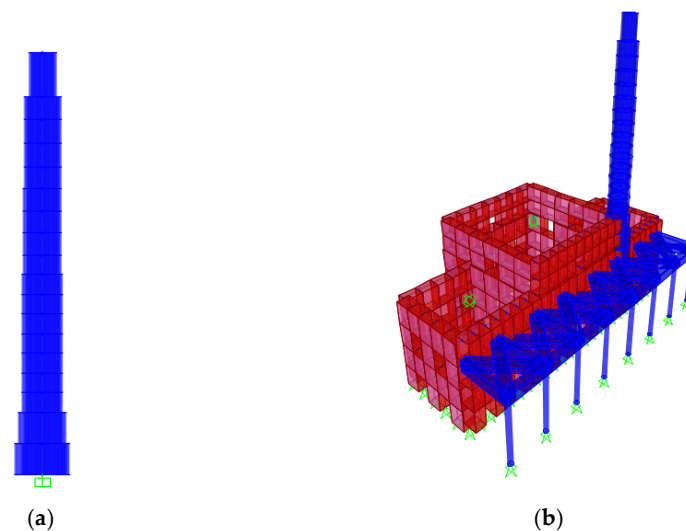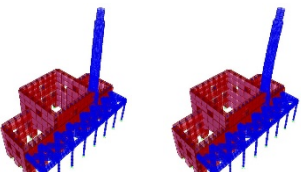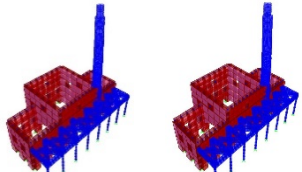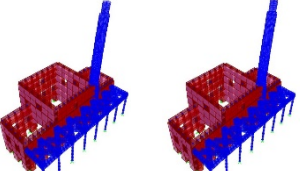

Figure 9. Modeling of (**a**) the minaret as a single cantilever column and (**b**) of the whole structure.

4.2. Modal Analyses

After the synthesis of the two primary models presented in Figure 9, the modal analyses followed. For the complete investigation and understanding of the minaret's dynamic behavior, different simulations were formed, modifying the most important input parameters. We considered six models. Model I, the simplest one, simulates the isolated minaret and ignores site effects, soil–structure interaction, and foundation flexibility. Model VI, the most complicated, concerns the mosque and the minaret and considers site effects, SSI, and foundation flexibility. More specifically, the studied models are the following:

- **Model I** includes the minaret isolated from the mosque. The internal staircase is simulated with elastic beam column elements with the minaret's masonry characteristics (Table 1). The fundamental frequency of construction for both the X–X and y–y directions is estimated at 1.55Hz (Table 3). As expected, due to the symmetry of the model, the first two frequencies are similar.
- **Model II** investigates the influence of the staircase material on the dynamic behavior of the minaret. In that direction, the staircase's elastic modulus is quadrupled compared to the utilized elastic modulus in Model I. From the modal analysis results (Table 3), it is understood that the modification of the staircase's elastic modulus does not significantly affect the minaret's dynamic characteristics.
- In **Model III,** the staircase's linear beam elements are removed. Their weight is simulated by increasing the specific unit weight of the masonry proportionally. Again, the eigenperiods and the modes are not significantly affected (Table 3).
- **Model IV** simulates the whole mosque. Thus, it investigates the minaret's behavior in conjunction with the underlying construction of the mosque. The structure is fixed at its base.
- **Model V** simulates the whole structure again, but it also considers soil–structure interactions with appropriate vertical and horizontal springs at the foundation level nodes, assuming a rigid foundation [62]. As we simulated the soil using appropriate static, linear elastic springs according to Gazetas, 1983, the only parameter we needed for the soil was the shear-wave velocity V_s for the first 30 m of the soil profile and Poisson's ratio v, which is considered herein equal to 0.33 (see Section 2.4).
- **Model VI**, except for soil–structure interactions, also considers the foundation flexibility using appropriate reduction factors of rigid foundation stiffness as proposed in [63].

Table 3. Comparison of the considered numerical FEMs of the monument and the experimental results using the SSI method (f: frequency).

Model	Numerical Model Mode Shape f (Hz)	Experimental Model f (Hz)	MAC for 1st Mode for 2nd Mode
I	$f_1 = f_2 = 1.55$ Translational along the longitudinal (left)–transverse (right) direction and torsional		0.95 0.93
II	$f_1 = f_2 = 1.59$ Translational along the transverse (left)–longitudinal (right) direction and torsional		0.86 0.83
III	$f_1 = f_2 = 1.55$ Coupled translational along the longitudinal (left)–transverse (right) direction and torsional	$f_1 = 1.63$ $f_2 = 1.80$	0.99 1.00
IV	$f_1 = f_2 = 1.53$ Coupled translational and torsional		1.00 1.00
V	$f_1 = f_2 = 1.52$ Coupled translational and torsional		0.88 0.84
VI	$f_1 = f_2 = 1.52$ Coupled translational and torsional		0.81 0.77

In the isolated minaret (Models I–III) case, the internal staircase's contribution is negligible. It can be omitted from the simulation by (i) distributing its weight in the minaret model, (ii) modifying the gravity of the finite elements, or by (iii) applying an extra load. For all six models, there is no significant difference in the first two periods of the minaret, which shows that the minaret's response is slightly affected by the presence of the underlying construction. Due to symmetry, the first and second frequencies and the third and fourth frequency values of the minaret are almost the same, which is also observed by Bayraktar and Hokelekli [64]. We decided to present only the first two eigenfrequencies from the modal analyses, as, for the cases in which the whole mosque is simulated, the third and fourth frequency values of the minaret were found to be subsequent frequencies of the whole model.

A validation of the whole mosque was conducted by comparing the natural period of the mosque (third eigenperiod, as the first two corresponded to the minaret) with the simple empirical relation for masonry mosques' natural period proposed by Ashayeri et al. [65]. According to this relationship and the characteristics of the mosque, the predicted value for the period T is estimated to be equal to 0.27 s. This value is very close (about 4% lower) to the estimated one for Model V (T = 0.28 s) which simulates the whole structure considering soil–structure interactions. Concerning the minaret, we verified the modal analysis results in the following ways. First, using the HVSR method, the minaret's measured frequency was estimated to be equal to 1.63 Hz. From the various numerical models of the minaret (Models I–III) the frequencies resulted in the range of 1.55–1.59 Hz (from 2% up to 5% lower compared to the estimated frequency with the HVSR), while from the experimental analyses using the SSI method, the frequencies were estimated in the range of 1.63–1.80 Hz (from 0% up to 10% higher compared to the estimated frequency with the HVSR). Chatzidakis et al. [45], who performed numerical analyses before the restoration of the minaret that took place in 2005, found a fundamental frequency for the minaret equal to 1.7 Hz. It is obvious that all estimated frequencies are in good agreement.

4.3. Comparison Between the Analytical and the Experimental Modal Analysis Results

The experimental modal identification results presented in Section 3 define the monument's optimal numerical models that reflect the measured dynamic response. The selection of the "best" model was made based on the evaluation of the modal assurance criterion (MAC) [66] for the identified modes quantified as:

$$MAC_{ij} = \frac{\left(\varphi_j^T \varphi_{Ei}\right)}{\left(\varphi_j^T \varphi_i\right)\left(\varphi_{Ej}^T \varphi_{Ei}\right)} \tag{1}$$

where φ_j is the eigenvector j from the numerical model and φ_{Ei} the eigenvector i from the field monitoring test (experimental model). Due to the simple dynamic response of minarets, MAC results from two nodes are representative of the quality of the numerical models.

The computation of the MAC values and the correlation of the experimental and numerical modal models' responses are made at two nodes for the minaret (one node per floor at the minaret corresponding to the sensor locations). A good correlation between the two tested modes is considered to be achieved for MAC values greater than 0.8. Indicatively, in Table 3, the modal analyses of the considered numerical finite element models of the monument are compared with the SSI method's experimental results. In general, it is seen that high MAC values are obtained for the structural modes of interest, indicating a perfect correlation between the experimentally and numerically derived mode shapes. Based on the MAC results, almost all the models correlate well with the experimental results for the modes under investigation (MAC > 0.8).

Moreover, the comparison of the experimental results with finite element models (FEMs) in terms of eigenfrequencies presented in Table 4 indicated that the experimental results give about 1.9–7.9% higher frequencies for the first mode. In contrast, for the second mode, the observed frequencies are almost 11.7–16.5% higher.

Table 4. Deviation of the eigenfrequencies between the experimental models and FEMs.

Model	Deviation (%)
I	4.3–6.1
	13.9–14.8
II	1.9–3.6
	11.7–12.6
III	4.3–6.1
	13.9–14.8
IV	5.6–7.3
	15.0–15.9
V	6.2–7.9
	15.6–16.5
VI	6.2–7.9
	15.6–16.5

4.4. Summary of the Results

From the modal analyses it is seen that due to symmetry, the first and second frequency values and the third and fourth frequency values of the minaret are almost the same. It is noted that for the cases that the whole mosque is simulated, the third and fourth frequency values of the minaret are found to be subsequent frequencies of the whole model. In general, for all six models, the minaret responds independently from the rest structure, implying that it could be simulated alone, without the rest of the underlying building.

Regarding the HVSR method, there are several studies in the literature [67,68] which prove that it is able to detect building fundamental modes and frequencies. These studies verified the suitability of the horizontal-to-vertical spectral ratio (HVSR) for estimating the dynamic characteristics of buildings when only single station seismic noise measurements are available. This verification is also achieved in the present study. Using the HVSR method, the minaret's measured frequency is 1.63 Hz. From the various numerical models of the minaret (Models I–III) the frequencies are in the range of 1.55–1.59 Hz, while from the experimental analyses using the SSI method the frequencies are 1.63–1.80 Hz. The differences in terms of frequencies are up to 10%.

Regarding the MAC values presented in Table 3, we observe that they are high (>0.8), indicating a perfect correlation between the experimentally and numerically derived mode shapes. Thus, almost all the models correlate well with the experimental results for the modes under investigation.

Finally, the comparison of the experimental results with the FEMs in terms of eigenfrequencies shows that the experimental results give about 1.9–7.9% higher frequencies for the first mode, while for the second mode, the observed frequencies are almost 11.7–16.5% higher. Therefore, it can be concluded that the finite element models are reliable to evaluate the actual mode shapes and eigenfrequencies of the minarets and thus to evaluate the response of the minarets to potential ground motions in future earthquakes.

The present paper provides solid evidence of the unique dynamic response of soil–mosque–minaret systems, using both numerical and experimental data, highlighting the effect of the soil in the dynamic response.

5. Conclusions

The present paper examines the dynamic system identification of the minaret of the Suleiman Mosque located in the medieval city of Rhodes, Greece. First, we performed sets of ambient vibration measurements at the minaret of the monument. Based on these data, we calculated the eigenproperties of the minaret. Next, we modeled the monument in

three dimensions, using the finite element method. Six numerical models were considered. Model I is the simplest one (isolated, fixed base minaret). Model VI is the most complicated one (simulation of the whole mosque and considering soil–structure interactions and foundation flexibility). Our primary goal was to verify the efficiency of the gradually more complicated numerical models against system identification of the dynamic characteristics from ambient noise measurements. The main conclusions are the following:

- We conclude that all six numerical models approach the fundamental eigenfrequencies of the actual construction that resulted from the experimental field measurements.
- Secondly, from the parametric analyses, the soil–structure interactions and the foundation flexibility do not significantly affect the minaret's response in terms of the eigenperiods on the bases of the performed models.
- Additionally, we conclude that the seismic response of a minaret, which is a high and flexible masonry structure, and part of a mosque with bulky and relatively rigid elements, is independent of the underlying construction. Thus, it could be simulated alone, without the rest of the underlying building.
- Finally, the simulation of the internal staircase does not affect the dynamic characteristics of the construction. The fundamental eigenvalues are slightly modified. The same conclusion regarding the internal staircase simulation's influence is reached by Oliveira et al. [69].

Author Contributions: Conceptualization, A.K. and D.P.; Data curation, A.K. and D.P.; Investigation, A.K., D.P. and S.K.; Methodology, A.K., D.P. and S.K.; Software, A.K. and S.K.; Supervision, D.P.; Writing—original draft, A.K.; Writing—review & editing, D.P. and S.K. All authors have read and agreed to the published version of the manuscript.

Conflicts of Interest: The authors declare no conflict of interest.

References

1. Betti, M.; Galano, L.; Vignoli, A. Finite element modelling for seismic assessment of historic masonry buildings. In *Earthquakes and Their Impact on Society*; D'amico, S., Ed.; Springer: Berlin/Heidelberg, Germany, 2016; pp. 377–415.
2. Gentile, C.G.; Saisi, A. One-year dynamic monitoring of a historic tower: Damage detection under changing environment. *Meccanica* **2016**, *51*, 2873–2889. [CrossRef]
3. Ubertini, F.; Cavalagli, N.; Kita, A.; Comanducci, G. Assessment of a monumental masonry bell-tower after 2016 Central Italy seismic sequence by long-term SHM. *Bull. Earthq. Eng.* **2018**, *16*, 775–801. [CrossRef]
4. Azzara, R.M.; Girardi, M.; Padovani, C.; Pellegrini, D. Experimental and numerical investigations on the seismic behaviour of the San Frediano bell tower in Lucca. *Ann. Geophys.* **2019**, *61*, 59. [CrossRef]
5. Cuadra, C.; Karkee, M.B.; Tokeshi, K. Earthquake risk to Inca's historical constructions in Machupicchu. *Adv. Eng. Softw.* **2008**, *39*, 336–345. [CrossRef]
6. Casolo, S.; Sanjust, C.A. Seismic analysis and strengthening design of a masonry monument by a rigid body spring model: The "Maniace Castle" of Syracuse. *Eng. Struct.* **2009**, *31*, 1447–1459. [CrossRef]
7. Ogawa, J.; Cuadra, C.; Karkee, M.B.; Rojas, J. A study on seismic vulnerability of Inca's constructions. In Proceedings of the 4th International Conference on Computer Simulation in Risk Analysis and Hazard Mitigation, Risk Analysis IV, Rhodes, Greece, 27–29 September 2004; pp. 3–12.
8. Karatzetzou, A.; Negulescu, C.; Manakou, M.; François, B.; Seyedi, D.M.; Pitilakis, D.; Pitilakis, K. Ambient vibration measurements on monuments in the Medieval City of Rhodes, Greece. *Bull. Earthq. Eng.* **2015**, *13*, 331–345. [CrossRef]

9. Peña, F.; Lourenco, P.; Mendes, N.; Oliveira, D.V. Numerical models for the seismic assessment of an old masonry tower. *Eng. Struct.* **2010**, *32*, 1466–1478. [CrossRef]

10. D'Ambrisi, A.; Mariani, V.; Mezzi, M. Seismic assessment of a historical masonry tower with nonlinear static and dynamic analyses tuned on ambient vibration tests. *Eng. Struct.* **2012**, *36*, 210–219. [CrossRef]

11. Aras, F.; Krstevska, L.; Altay, G.; Tashkov, L. Experimental and numerical modal analyses of a historical masonry palace. *Constr. Build. Mater.* **2011**, *25*, 81–91. [CrossRef]

12. Ramos, L.F.; Lourenço, P.B.; Costa, A.C. Operational modal analysis for damage detection of a masonry construction. In Proceedings of the 1st International Operational Modal Analysis Conference, Copenhagen, Denmark, 24–26 April 2005; pp. 495–502.

13. Ramos, L.F.; Marques, L.; Lourenço, P.B.; De Roeck, G.; Campos-Costa, A.; Roque, J. Monitoring historical masonry struc-tures with operational modal analysis: Two case studies. *Mech. Syst. Signal Proc.* **2010**, *24*, 1291–1305. [CrossRef]

14. Proaño, R.; Scaletti, H.; Zavala, C.; Olarte, J.; Quiroz, L.; Castro Cuba, M.; Lazares, F.; Rodriguez, M. Seismic vulnerability of Lima cathedral, PERU. In Proceedings of the Conferencia International en Ingenieriasismica, Lima, Peru, 18–21 October 2007.

15. Fallahi, A.; Miyajima, M. Microtremor measurments in the affected area of the Changureh-avaj, Iran earthquake of June, 2002. In Proceedings of the 13th World Conference on Earthquake Engineering, Vancouver, BC, Canada, 1–6 August 2004; p. 159.

16. Horike, M. Inversion of phase velocity of long-period microtremors to the S-wave-velocity structure down to the basement in urbanized areas. *J. Phys. Earth* **1985**, *33*, 59–96. [CrossRef]

17. Apostolidis, P.; Raptakis, D.; Roumelioti, Z.; Pitilakis, K. Determination of S-wave velocity structure using microtremors and spac method applied in Thessaloniki (Greece). *Soil Dyn. Earthq. Eng.* **2004**, *24*, 49–67. [CrossRef]

18. Apostolidis, P.; Raptakis, D.; Pandi, K.; Manakou, M.; Pitilakis, K. Definition of subsoil structure and preliminary ground response in Aigion city (Greece) using microtremor and earthquakes. *Soil Dyn. Earthq. Eng.* **2006**, *26*, 922–940. [CrossRef]

19. Manakou, M.; Raptakis, D.; Chávez-García, F.; Apostolidis, P.; Pitilakis, K. 3D soil structure of the Mygdonian basin for site response analysis. *Soil Dyn. Earthq. Eng.* **2010**, *30*, 1198–1211. [CrossRef]

20. Reynders, E. System identification methods for (operational) modal analysis: Review and comparison. *Arch. Comput. Methods Eng.* **2012**, *19*, 51–124. [CrossRef]

21. Ventura, C.; Finn, W.L.; Lord, J.-F.; Fujita, N. Dynamic characteristics of a base isolated building from ambient vibration measurements and low level earthquake shaking. *Soil Dyn. Earthq. Eng.* **2003**, *23*, 313–322. [CrossRef]

22. Bindi, D.; Petrovic, B.; Karapetrou, S.; Manakou, M.; Boxberger, T.; Raptakis, D.; Pitilakis, K.D.; Parolai, S. Seismic response of an 8-story RC-building from ambient vibration analysis. *Bull. Earthq. Eng.* **2014**, *13*, 2095–2120. [CrossRef]

23. Pitilakis, K.; Karapetrou, S.; Bindi, D.; Manakou, M.; Petrovic, B.; Roumelioti, Z.; Boxberger, T.; Parolai, S. Structural monitoring and earthquake early warning systems for the AHEPA hospital in Thessaloniki. *Bull. Earthq. Eng.* **2016**, *14*, 2543–2563. [CrossRef]

24. Karapetrou, S.; Manakou, M.; Bindi, D.; Petrovic, B.; Pitilakis, K. "Time-building specific" seismic vulnerability assessment of a hospital RC building using field monitoring data. *Eng. Struct.* **2016**, *112*, 114–132. [CrossRef]

25. Michel, C.; Guguen, P.; Causse, M. Seismic vulnerability assessment to slight damage based on experimental modal pa-rameters. *Earthq. Eng. Struct. Dyn.* **2012**, *41*, 81–98. [CrossRef]

26. De Silva, F.; Pitilakis, D.; Ceroni, F.; Sica, S.; Silvestri, F. Experimental and numerical dynamic identification of a historic masonry bell tower accounting for different types of interaction. *Soil Dyn. Earthq. Eng.* **2018**, *109*, 235–250. [CrossRef]

27. Milani, G.; Casolo, S.; Naliato, A.; Tralli, A. Seismic assessment of a medieval masonry tower in northern italy by limit, nonlinear static, and full dynamic analyses. *Int. J. Arch. Heritage* **2012**, *6*, 489–524. [CrossRef]

28. Casolo, S.; Milani, G.; Uva, G.; Alessandri, C. Comparative seismic vulnerability analysis on ten masonry towers in the coastal Po Valley in Italy. *Eng. Struct.* **2013**, *49*, 465–490. [CrossRef]

29. Bayraktar, A.; Altunişik, A.; Muvafik, M. Damages of minarets during Erciş and Edremit earthquakes, 2011 in Turkey. *Smart Struct. Syst.* **2014**, *14*, 479–499. [CrossRef]

30. Şahin, A.; Bayraktar, A.; Özcan, D.M.; Sevim, B.; Altunışık, A.C.; Türker, T. Dynamic field test, system identification, and modal validation of an RC Minaret: Preprocessing and post-processing the wind-induced ambient vibration data. *J. Perform. Constr. Facil.* **2011**, *25*, 336–356. [CrossRef]

31. Osmancikli, G.; Uçak, Ş.; Turan, F.N.; Türker, T.; Bayraktar, A. Investigation of restoration effects on the dynamic charac-teristics of the Hagia Sophia bell-tower by ambient vibration test. *Constr. Build. Mater.* **2012**, *29*, 564–572. [CrossRef]

32. Bayraktar, A.; Calik, İ.; Turker, T.; Ashour, A. Restoration effects on experimental dynamic characteristics of masonry stone minarets. *Mater. Struct.* **2018**, *51*, 141. [CrossRef]

33. Bernardeschi, K.; Padovani, C.; Pasquinelli, G. Numerical modelling of the structural behaviour of Buti's bell tower. *J. Cult. Heritage* **2004**, *5*, 371–378. [CrossRef]

34. Bayraktar, A.; Şahin, A.; Özcan, D.M.; Yildirim, F. Numerical damage assessment of Haghia Sophia bell tower by nonlinear FE modeling. *Appl. Math. Model.* **2010**, *34*, 92–121. [CrossRef]

35. Forcellini, D.; Giardi, F.; Tanganelli, M. Seismic assessment of the historical third tower in San Marino based on a 3D laser scanner survey (3D-LSS). *Innov. Infrastruct. Solut.* **2019**, *4*, 20. [CrossRef]

36. Karatzetzou, A.; Pitilakis, D. Reduction factors to evaluate acceleration demand of soil-foundation-structure systems. *Soil Dyn. Earthq. Eng.* **2018**, *109*, 199–208. [CrossRef]

37. Karafagka, S.; Fotopoulou, S.; Pitilakis, D. Fragility assessment of non-ductile RC frame buildings exposed to combined ground shaking and soil liquefaction considering SSI. *Eng. Struct.* **2021**, *229*, 111629. [CrossRef]

38. Karatzetzou, A.; Pitilakis, D.; Kržan, M.; Bosiljkov, V. Soil–foundation–structure interaction and vulnerability assessment of the Neoclassical School in Rhodes, Greece. *Bull. Earthq. Eng.* **2015**, *13*, 411–428. [CrossRef]
39. Cattari, S.; Lagomarsino, S.; Karatzetzou, A.; Pitilakis, D. Vulnerability assessment of Hassan Bey's Mansion in Rhodes. *Bull. Earthq. Eng.* **2014**, *13*, 347–368. [CrossRef]
40. Hökelekli, E.; Al-Helwani, A. Effect of soil properties on the seismic damage assessment of historical masonry minaret–soil interaction systems. *Struct. Des. Tall Spéc. Build.* **2019**, *29*, e1694. [CrossRef]
41. Mitropoulou, C.C.; Kostopanagiotis, C.; Kopanos, M.; Ioakim, D.; Lagaros, N.D. Influence of soil–structure interaction on fragility assessment of building structures. *Structures* **2016**, *6*, 85–98. [CrossRef]
42. Forcellini, D. Analytical fragility curves of shallow-founded structures subjected to Soil-Structure Interaction (SSI) effects. *Soil Dyn. Earthq. Eng.* **2021**, *141*, 106487. [CrossRef]
43. Finn, W.D.L. A study of piles during earthquakes: Issues of design and analysis. *Bull. Earthq. Eng.* **2005**, *3*, 141–234. [CrossRef]
44. Cavalieri, F.; Correia, A.A.; Crowley, H.; Pinho, R. Seismic fragility analysis of URM buildings founded on piles: Influence of dynamic soil–structure interaction models. *Bull. Earthq. Eng.* **2020**, *18*, 4127–4156. [CrossRef]
45. Chatzidakis, A.; Moschouris, P.; Nistikouli, A. *Restoration of Suleyman Mosque in the medieval city of Rhodes*; University Studio Press: Thessaloniki, Greece, 2002.
46. Dellas, G.; Vlysides, S.; Stefanis, A. *The Restoration of Suleiman Mosque in the Medieval Town of Rhodes*; University Studio Press: Thessaloniki, Greece, 2009. (In Greek)
47. Chronopoulos, M. *Study of Structural Materials (Mortars—Grouts)*; Technical Report; National Technical University: Athens, Greece, 1991. (In Greek)
48. Pitilakis, K. *Stability Issues of the Foundation of the Fortification of the Medieval City of Rhodes*; Technical report (in Greek). Laboratory of Soil Mechanics, Foundation & Geotechnical Earthquake Engineering; Civil Engineering Department; Aristotle University of Thessaloniki: Thessaloniki, Greece, 1998.
49. Manakou, M.; Pitilakis, K.; Karatzetzou, A.; Riga, E.; Kotlida, D.; Stais, V. Results of in-situ Microtremors Surveys and Array Measurements at Selected Sites, PERPETUATE (EU-FP7 Research Project), Deliverable D18. 2011. Available online: http://www.perpetuate.eu (accessed on 30 June 2021).
50. CEN. *Eurocode 8: Design of Structures for Earthquake Resistance—Part 1: General Rules, Seismic Actions and Rules for Buildings, European Standard EN 1998-1:2004*; European Committee for Standardisation: Brussels, Belgium, 2004.
51. Ljung, L. *System Identification—Theory for the User*, 2nd ed.; PTR Prentice Hall: Upper Saddle River, NJ, USA, 1999.
52. Lagomarsino, S.; Modaressi, H.; Pitilakis, K.; Bosiljkov, V.; Calderini, C.; D'Ayala, D.; Benouar, D.; Cattari, S. PERPETUATE project: The proposal of a performance-based approach to earthquake protection of cultural heritage. *Adv. Mater. Res.* **2010**, *133-134*, 1119–1124. [CrossRef]
53. Nakamura, Y. A method for dynamic characteristics estimation of subsurface using microtremors on the ground surface. *QR Railway Tech. Res. Inst.* **1989**, *30*, 1.
54. Pitilakis, K. *Site Effects, Recent Advances in Earthquake Geotechnical Engineering & Microzonation*; Ansal, A., Ed.; Springer: Asterdam, The Netherlands, 2004; pp. 139–197.
55. Van Overschee, P.; De Moor, B. Subspace algorithms for the stochastic identification problem. In Proceedings of the 30th IEEE Conference on Decision and Control, Brighton, UK, 11–13 December 2002; pp. 1321–1326.
56. Tolley, H.D.; Bendat, J.S.; Piersol, A.G. Engineering applications of correlation and spectral analysis. *J. Am. Stat. Assoc.* **1982**, *77*, 689. [CrossRef]
57. Brincker, R.; Zhang, L.; Andersen, P. Modal identification of output-only systems using frequency domain decomposition. *Smart Mater. Struct.* **2001**, *10*, 441–445. [CrossRef]
58. Reynders, E.; Schevenels, M.; De Roeck, G. *MACEC 3.3: A Matlab Toolbox for Experimental and Operational Modal Analy-Sis-User's Manual*; Katholieke Universiteit: Leuven, Belgium, 2014.
59. Elnashai, A.S.; Disarno, L. *Fundamentals of Earthquake Engineering*; Wiley: Hoboken, NJ, USA, 2008.
60. Rainieri, C.; Fabbrocino, G.; Cosenza, E. Some remarks on experimental estimation of damping for seismic design of civil constructions. *Shock. Vib.* **2010**, *17*, 383–395. [CrossRef]
61. Computers and Structures Inc. *SAP 2000-Structural Analysis Program: Linear and Nonlinear Static and Design of Three-Dimensional Structures*; Computers and Structures Inc.: Berkeley, CA, USA, 2004.
62. Gazetas, G. *Analysis of Machine Foundation Vibrations: State of the Art*; Rensselaer Polytechnic lnstitute: New York, NY, USA, 1983.
63. Pitilakis, D.; Karatzetzou, A. Dynamic stiffness of monumental flexible masonry foundations. *Bull. Earthq. Eng.* **2015**, *13*, 67–82. [CrossRef]
64. Bayraktar, A.; Hökelekli, E. Influences of earthquake input models on nonlinear seismic performances of minaret-foundation-soil interaction systems. *Soil Dyn. Earthq. Eng.* **2020**, *139*, 106368. [CrossRef]
65. Ashayeri, I.; Biglari, M.; Formisano, A.; D'Amato, M. Ambient vibration testing and empirical relation for natural period of historical mosques. Case study of eight mosques in Kermanshah, Iran. *Constr. Build. Mater.* **2021**, *289*, 123191. [CrossRef]
66. Allemang, R.J.; Brown, D.L. A correlation coefficient for modal vector analysis. In Proceedings of the 1st International Modal Analysis Conference, SEM, Orlando, FL, USA, 8–10 November 1982; pp. 110–116.

67. Gallipoli, M.R.; Mucciarelli, M.; Castro, R.R.; Monachesi, G.; Contri, P. Structure, soil–structure response and effects of damage based on observations of horizontal-to-vertical spectral ratios of microtremors. *Soil Dyn. Earthq. Eng.* **2004**, *24*, 487–495. [CrossRef]
68. Di Tommaso, R.; Parolai, S.; Mucciarelli, M.; Eggert, S.; Sobiesiak, M.; Zschau, J. Monitoring the response and the back-radiated energy of a building subjected to ambient vibration and impulsive action: The Falkenhof Tower (Potsdam, Germany). *Bull. Earthq. Eng.* **2009**, *8*, 705–722. [CrossRef]
69. Oliveira, C.S.; Çaktı, E.; Stengel, D.; Branco, M. Minaret behavior under earthquake loading: The case of historical Istanbul. *Earthq. Eng. Struct. Dyn.* **2011**, *41*, 19–39. [CrossRef]